ICANS-XIII
13th Meeting of the International Collaboration on
Advanced Neutron Sources
October 11-14, 1995
Paul Scherrer Institut, 5232 Villigen PSI, Switzerland

SMALL-ANGLE SCATTERING INSTRUMENTS ON A 1 MW LONG PULSE SPALLATION SOURCE

Glenn A. Olah *, Rex P. Hjelm † and Phil A. Seeger ‡

* Biosciences and Biotechnology Group, Chemical Science and Technology Division, Los Alamos National Laboratory, Los Alamos, NM 87545 USA
† Neutron Scattering Center, Los Alamos Neutron Science Center, Los Alamos National Laboratory, Los Alamos, NM, 87575 USA
‡ 239 Loma del Escolar, Los Alamos, NM 87544 USA

ABSTRACT

We have designed and optimized two small-angle neutron scattering instruments for installation at a 1 MW long pulse spallation source. The first of these instruments measures a Q-domain from 0.002 to 0.44 $Å^{-1}$, and the second instrument from 0.00069 - 0.17 $Å^{-1}$. Design characteristics were determined and optimization was done using a Monte Carlo instrument simulation package under development at Los Alamos. A performance comparison was made between these instruments with D11 at the ILL by evaluating the scattered intensity and rms resolution for the instrument response function at different Q values for various instrument configurations needed to span a Q-range of 0.0007 - 0.44 $Å^{-1}$. We concluded that the first of these instruments outperforms D11 in both intensity and resolution over most of the Q-domain and that the second is comparable to D11. Comparisons were also made of the performance of the optimized long pulse instruments with different reflectors and with a short pulse source, from which we concluded that there is an optimal moderator-reflector combination, and that a short pulse does not substantially improve the instrument performance.

1. Introduction

Small-angle neutron scattering (SANS) allows structural studies on length scales from about 10 to 1000 Å. The unique characteristics of neutron radiation give certain advantages over other types of radiation. For example, differences in scattering length between elements of similar atomic number and between different isotopes of the same element provide unique experimental capabilities. Varying the scattering contrast in polymeric and biological materials by selective deuteration in solvents and molecular subunits has led to information on the conformation of macromolecules unobtainable by any other technique. Neutron penetrability enables the application of SANS to nondestructive evaluation of nanoscale structure and in *in situ* measurements of samples in extreme environments requiring containment. All of these factors make SANS an indispensable tool in biological, chemical, physical and engineering research. It is therefore desirable to build SANS instruments on any high flux neutron source.

Keywords: SANS, Simulations, Monte Carlo, MCLIB, Long Pulse

We have begun evaluation of a new 1 MW long pulse spallation source (LPSS). At a recent workshop at Lawrence Berkeley National Laboratory [1], the panel on SANS instrumentation specified four characteristics of modern SANS instrumentation to meet the needs of emerging science. 1) A momentum transfer, Q, domain covering 0.5 to 0.001 $Å^{-1}$. ($Q = 4\pi\sin\theta/\lambda$, were θ is half the scattering angle from the incident beam and λ is the neutron wavelength.) 2) The ability to vary resolution, $\sigma(Q)/Q$ (rms), from no greater than 2% to 15%. 3) The ability to use different sample sizes and geometries. 4) The instruments should have low backgrounds.

In this report, we show the design and optimization of two LPSS-SANS instruments, which span the Q-domain from 0.0007 - 0.44 $Å^{-1}$. These include the Basic Low-Q Diffractometer (BLQD), which spans the Q-domain 0.002 to 0.44 $Å^{-1}$, and the Very Low-Q Diffractometer (VLQD), which spans the Q-domain 0.00069 - 0.17 $Å^{-1}$. These two proposed instruments meet the majority of requests made by participants from the Berkeley workshop [1]. We also characterize the performance of these instruments including a comparison with one of the world standards for SANS instruments, the 'as-built' D11 at the ILL in Grenoble, France.

2. Methods

Requirements for increased neutron flux, improved resolution, and a wider Q-range drive the designs of new SANS instrumentation and their sources of neutrons. A 1 MW long pulse source will provide long wavelength neutron fluxes considerably higher than that obtained at present day spallation sources, with average fluxes comparable to some present day reactors. In this paper we optimize the instruments for a case where the source is a 1 ms proton pulse operating at a frequency of 60 Hz. The total power dissipated on the tungsten target is 1 MW. We use the calculated brilliance ($n/cm^2/sterad/eV$) for a liquid H_2 moderator fully coupled with a reflector composed of 60 cm of Be surrounded by another 90 cm of Pb. The

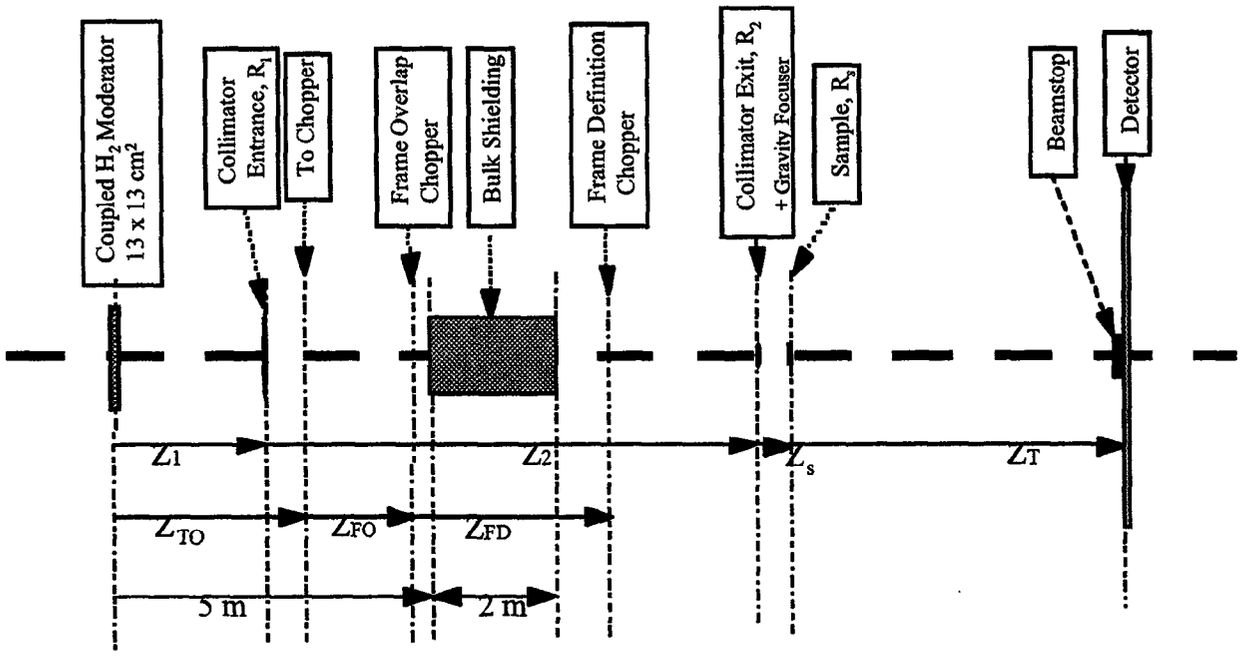

Figure 1. Schematic of simulated components for LPSS small-angle instrument. Bulk shielding was assumed fixed between 5 and 7 m from the moderator. A box will be located between 2.5 and 5 m which can house the T_0 and frame overlap choppers (and an additional chopper if necessary).

spectrum and pulse shape characteristics of the coupled moderator and reflector system were those calculated by Pitcher *et al.* using the Monte Carlo Nuclear Particle Transport code, MCNP [2]. Design characteristics were determined and optimization was done using the Monte Carlo instrument simulation package [3] under development at Los Alamos, which is based on the MCLIB Monte Carlo library originally developed at the Rutherford Laboratory [4]. The strongly coupled liquid hydrogen moderator 60 cm Be-90 cm Pb reflector source has a long tail in the low energy pulse structure characterized by a exponential decay with a time constant of 0.734 ms. Although these strongly coupled systems provide greater peak and integrated fluxes than more weakly coupled systems with shorter pulse tails, we must carefully consider the effects of the pulse tails on the instrument response function.

SANS instrument design used on the LPSS, like all SANS instruments, is inherently simple, consisting of a neutron source, a collimation system, choppers, shielding, and position sensitive detectors, see Figure 1. Instrument design and optimization for pulsed sources depends on obtaining as large a wavelength band width as possible (to maximum gains due to the use of time-of-flight (TOF) techniques) consistent with avoiding frame overlap. The first step taken in the instrument design involves the determination of the number and location of choppers, an initial assessment of which was done using a time-distance graphical utility developed by Luc Daemen at Los Alamos. The main objective of the chopper system is to define the wavelength bandwidth and to eliminate out of frame neutrons. System performance was evaluated by simulating a δ scatterer at fixed Q, and optimal configurations were determined by maximizing a figure of merit, FOM, which measures how long an experiment takes to get the same quality data

$$FOM = \frac{I(Q)}{V[Q]} \ln\left(\frac{Q_{\max}}{Q_{\min}}\right)$$

Parameters are chosen to give nearly the same value of the variance, V[Q], then the scattered intensity mapped into Q-space, I(Q), is compared. The logarithm of the Q-range represents the number of channels mapped into logarithmic Q-bins in a single instrument configuration. Resolution, $\sqrt{V(Q)}$, was calculated from the instrument response function determined from the scattering profile from the hypothetical δ scatterer. Thus the optimization is to maximize the count rate at fixed resolution. The maximum intensity of the instrument response function is dependent on the sample transmission which was assumed to vary as $\exp(-\alpha\lambda)$ and which was arbitrarily set at 68% for 10 Å neutrons. Here, the SANS instruments were designed and optimized by fixing the minimum desired Q at 0.0025 $Å^{-1}$ for the BLQD and at 0.0008 $Å^{-1}$ for the VLQD. For the fixed Q of the δ scatterer $\sigma(Q)/Q$ is fixed at 10%. Instrument optimization and performance simulations [2,5,6] included source energy and time structure, shielding location, wavelength-dependent effects from aluminum in the beam, chopper location, chopper opening and closing times and phase jitter, sample transmission and multiple scattering, and gravity.

3. Results

3.1. Basic Design Considerations and Optimization

Instrument designs used in this study take into account the current design of the target monolith shield. This includes a chopper box located between 2.5 and 5 m from the moderator can

house the T_0 and frame overlap choppers. Bulk shielding is placed between 5 and 7 m. We used single pinhole collimation with the entrance aperture located at 2.5 m from the moderator for both BLQD and VLQD. The exit aperture is 20 mm in front of the sample.

We have assumed in this report that large-area (1 m x 1 m) detectors with fast encoding will be available with 5 mm square pixels (and 3.4 mm resolution). For simulations of the BLQD and VLQD, two 1m x 1m detectors were used with one detector placed 0.25 m off-axis, and a second detector placed 0.75 m off-axis to extend the dynamic range.

We found that three choppers are needed to eliminate out of frame neutrons. A massive T_0 chopper eliminates the initial burst of high-energy neutrons and must block these fast neutrons over the total 13 cm x 13 cm moderator size. The location, opening time and phase of the T_0 chopper is important for defining the total usable wavelength range. Placing the T_0 at 2.8 m from the moderator maximizes the range from 2.5 to 12.8 Å. This is particularly important since we have made the instrument short to maximize the TOF gain. Should it be that cost, engineering and maintenance require that the T_0 chopper be moved farther out from the source, then we would have to optimize to a longer total flight path, similar to the low-Q instrument discussed previously [1]. The frame overlap chopper, located at 4.8 m for BLQD and 4.2 m for VLQD , assures that fast neutrons in the tail of the following pulse cannot reach the detector. The location of this chopper limits the maximum usable wavelength; the closer it is to the T_0 chopper the longer the wavelength that can be used. With these positions, the maximum wavelength is 12.8 Å for BLQD and 14.8 Å for VLQD. A third chopper, the frame definition chopper defines the time frame (T_{min} and T_{max}) to be measured within the 60 Hz cycle. Its phase is adjusted to be half closed for the maximum wavelength to be recorded for neutrons emitted at t = 0; thus, defining T_{max}. The chopper does not open again until the tail

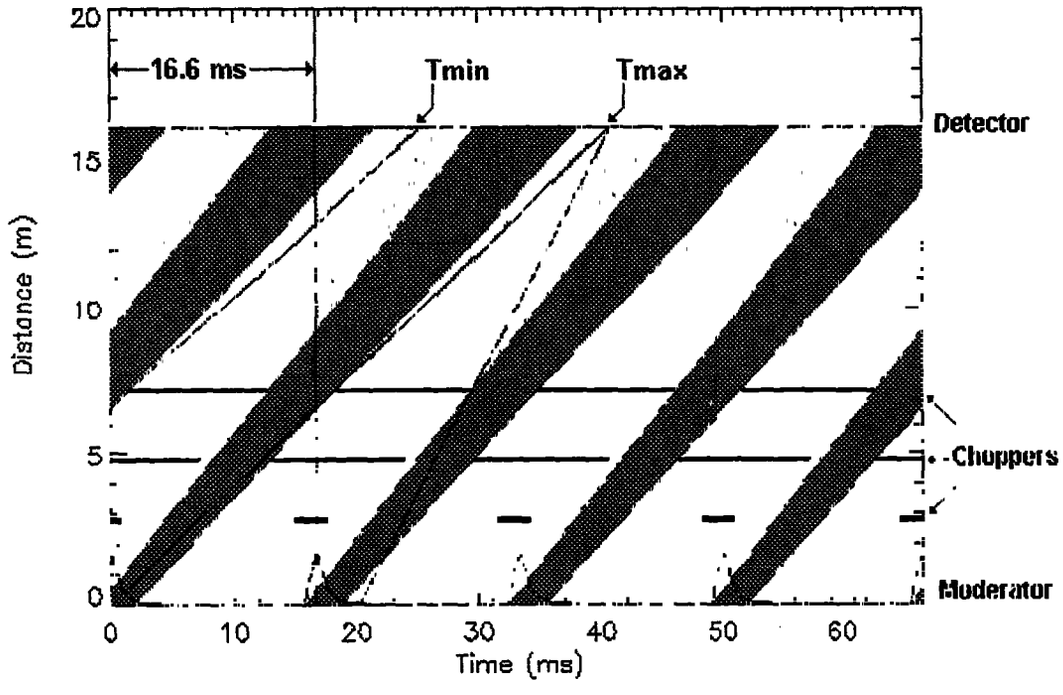

Figure 2. Distance-time diagram for BLQD showing the chopper phasing. The function of each of the choppers is defined in the text. Three lines represent choppers in the closed positions. The phasing shown gives neutrons from 6.4 Å to 10.2 Å.

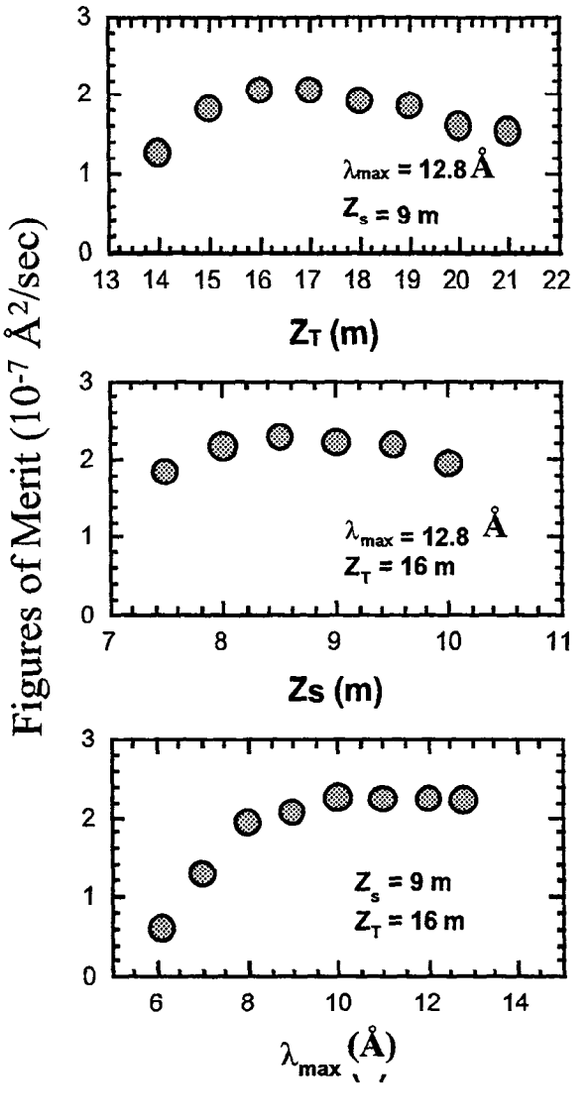

Figure 3. Parameter optimization for BLQD at Q = 0.01 Å^{-1}. The parameters Z_T, Z_s and λ_{max} were independently varied and the FOM calculated.

of the following pulse has decayed to 4.6 times the decay time constant to prevent frame overlap from neutrons originating in the tail of the following pulse. The T_{min} of the following pulse is defined by the delay after T_{max} after which we can guarantee that the frame definition chopper is fully closed (including three times the rms chopper jitter of 20 μs). The location of the frame definition chopper is important for blocking long wavelength (> 20 Å) out-of-frame neutrons from preceding pulses. Its optimal location depends on the location of the frame overlap chopper; therefore, positioning of the frame overlap and definition choppers requires an iterative process which depends on the T_{max} (or λ_{max}) desired. Figure 2 shows a distance-time diagram of the chopper configurations for the BLQD and a λ_{max} = 10.2 Å. In the unlikely event that long wavelength out of frame neutrons create background problems then these can be removed by placing a fourth chopper between the T_O and frame overlap chopper or by including a transmission Si mirror after the frame definition chopper.

The primary variables (see Figure 1) giving Q_{min} are the total instrument length, Z_T, the sample position, Z_s, and the maximum wavelength, λ_{max}. These values and the cone rule [7,8] give the sample radius, R_S, collimator entrance radius, R_1, collimator exit radius, R_2 , and the moderator penumbra radius, R_M. Z_T, Z_S and λ_{max} were independently varied and the figure of merit calculated. The results for BLQD are shown in Figure 3. The λ_{max} was fixed at 12.8 Å for both BLQD and VLQD when varying Z_T or Z_S. As Z_T is increased and with Z_S and λ_{max} fixed, a maximum in the figure of merit is reached. The figure of merit starts decreasing at larger Z_T due to the decrease in the usable wavelength band width and due to the decrease in the dynamic range. With Z_S and Z_T fixed and increasing λ_{max} , a plateau is reached at about 10 Å. For even larger wavelengths the resolution continues to improve but at the expense of dynamic range and incident flux. The Monte Carlo optimized parameters for the two instruments are given in Table 1. Possible layouts for BLQD and VLQD are given in Figure 4.

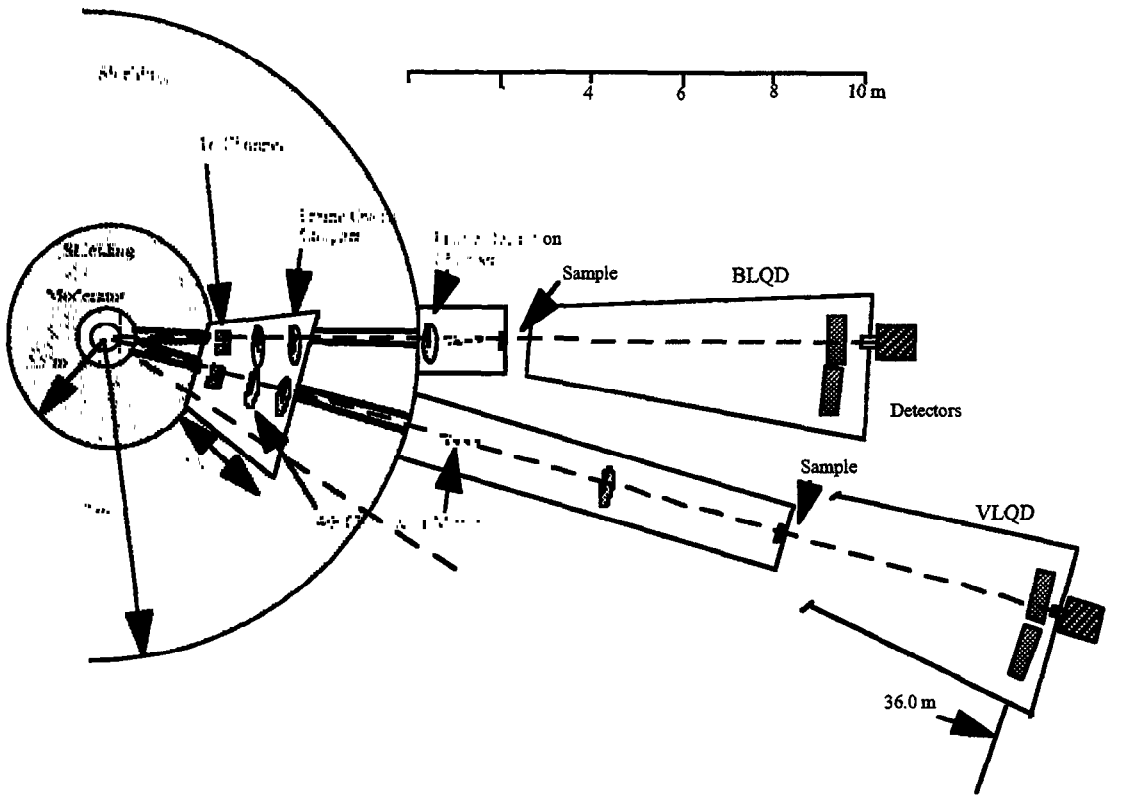

Figure 4. Possible layout for BLQD and VLQD.

Table 1
Optimized SANS Instruments

	Instrument	
Instrument Parameter	BLQD	VLQD
Moderator-reflector Time Constant (μs)	734	734
Moderator-to-Collimator Entrance, Z_1 (m)	2.5	2.5
Entrance Aperture Radius, R_1 (mm)	9.8 - 32.0	8.6
Moderator-to-To Chopper, Z_{To} (m)	2.8	2.8
Moderator-to-Overlap Chopper, Z_{FO} (m)	4.8	4.2
Moderator-to-Frame Chopper, Z_{FD} (m)	7.2	10.5
Moderator-to-Collimator Exit, Z_2 (m)	9	16
Exit Aperture Radius, R_2 (mm)	5.07	5.11
Moderator Phase Space (mster-mm^2)	570 - 6150	120
Gravity Focus Stroke (mm)	1.2	25
Sample Radius, Rs (mm)	5.07	5.11
Moderator-to-Sample, Z_s (m)	9.02	16.02
Sample-to-Detector (m)	6.98	19.98
Beamstop Radius (mm)	21	26
λ_{max} (Å)	12.8	14.8
Q_{min} (Å^{-1})	0.002	0.00069
λ_{min} (Å)	2.5	2.5
Q_{max} with One Detector (Å^{-1})	0.21	0.089
Q_{max} with Two Detectors (Å^{-1})	0.44	0.17

3.2. Comparison with 'as-built' D11

In this report, we decided to make an initial comparison between the two LPSS instruments and the 'as-built' D11. This was done since many SANS users are already familiar with the 'as-built' D11; and we have successfully made benchmarked simulation of D11 [5,6]. However, we plan eventually to make comparisons with simulated instruments 'optimized' on a reactor with a state of the art cold moderator, such as D22. 'As-built' means using the specifications given for D11 in reference [9] including an increase by a factor of two in flux due to the installation of the COSTANZE velocity selector. When comparing instruments, the two most important parameters to compare are the resolution and intensity, or preferably intensity at the same resolution.

In Figure 5, resolution in Q is shown for D11 at various sample-to-detector settings and for BLQD and VLQD. A minimum scattering angle θ_{min} can be estimated from a penumbra radius projected on the detector using the cone rule [7,8]. The minimum measurable Q for different settings was determined from the estimated θ_{min} and λ_{max}. We assumed a beamstop 2 mm larger in radius than the prenumbra size in determinining θ_{min}. Each box representing a

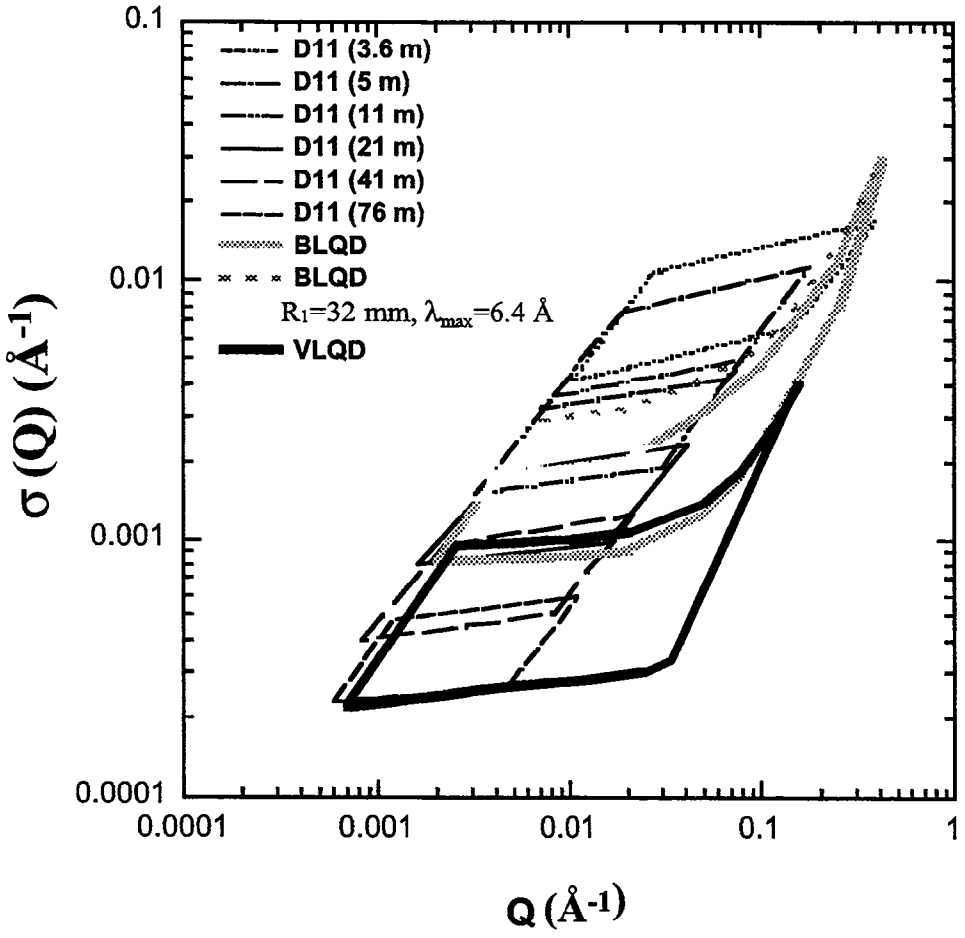

Figure 5. Comparison of resolution in Q for D11, BLQD and VLQD. The total collimation plus sample to detector distance is given in parentheses for D11. The sample to detector distance is half the total length except for the 3.6 and 76 m configurations in which case it is 1.1 m and 35.5 m, respectively.

D11 configuration corresponds to changing the velocity selector speed and thus selecting neutrons with different peak wavelengths between 4.5 and 12 Å. The 'as-built' D11 has a 64 cm x 64 cm area detector. Q_{max} of each box in Figure 5 was determined from the edge of this detector. Note that since the detector is flat, the resolution increases slightly as Q is increased for fixed wavelength. The boxes shown for BLQD and VLQD represent continuous choices of λ_{max}. BLQD can use wavelengths in the range from 2.5 to 12.8 Å and VLQD from 2.5 to 14.8 Å. Because TOF methods are used and the instruments are relatively short, slightly longer wavelengths can be used on the LPSS instruments.

Fair comparisons among different instruments consider scattering intensity mapped into Q-space using the same Q-precision and sample size in each case. The difference in detector size is dealt with below. Phase settings of choppers can be found for BLQD or VLQD that give the same resolution as D11 over roughly the same Q-range spanned by any one configuration of D11. We can begin making a comparison between D11 and the LPSS instruments by first asking the question: how would one measure the Q-range from 0.002 to 0.4 $Å^{-1}$ on D11? We then ask how would measurements on the LPSS instruments at the same resolution compare with the measurements on D11? As seen in Figure 6, three different sample-to-detector distances are required for D11 to measure this Q-range; namely, settings D11(21 m, 10 Å), D11(11 m, 5.5 Å) and D11(3.6 m, 4.5 Å), where the first number in parenthesis is Z_T and the second number is λ_O. BLQD at a phase setting of λ_{max} = 10 Å would have the same resolution as D11(21 m, 10 Å). This phase setting results in a factor of 2.8 more scattered intensity at any particular Q value between Q = 0.0025 - 0.018 $Å^{-1}$ relative to D11(21 m, 10 Å); how-

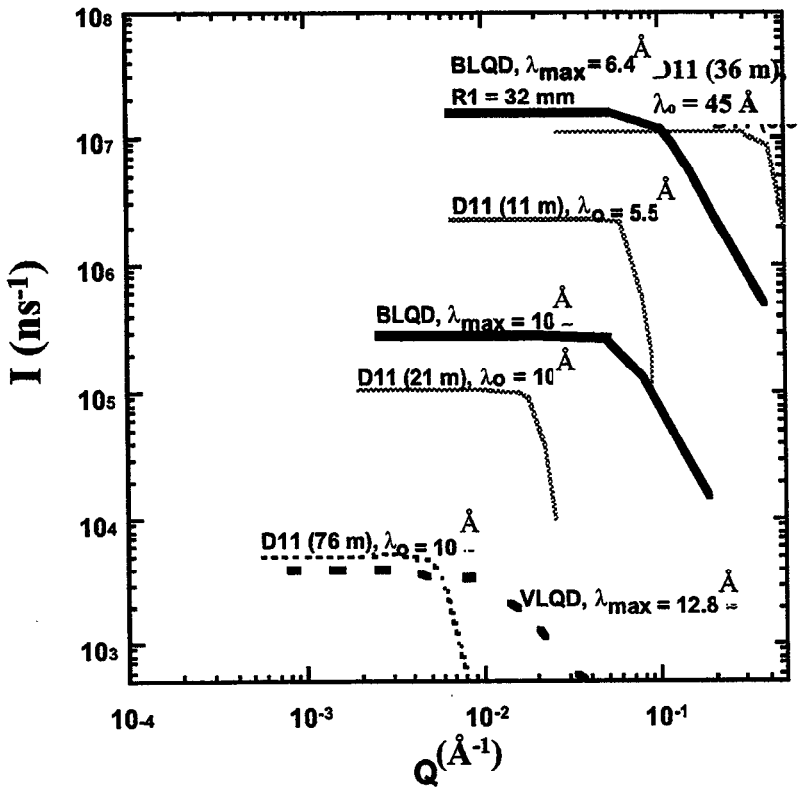

Figure 6. Comparison of scattered intensity for δ-scatterers for D11, BLQD and VLQD.

ever, LPSS does not reach a Q_{min} of 0.002 $Å^{-1}$. If a phase setting of λ_{max} = 12.8 Å is used then we obtain Q_{min} = 0.002 $Å^{-1}$, 30% better resolution and approximately the same scattered intensity. BLQD at the lowest wavelength phase setting of λ_{max} = 6.4 Å has approximately 23% better resolution than D11(11 m, 5.5 Å) but 30% less intensity. We can gain intensity at the expense of resolution by opening up the collimation entrance aperture R_1. The same resolution is obtained as D11 (11 m, 5.5 Å) over the Q-range 0.007-0.06 $Å^{-1}$ for R_1 = 32 mm. This BLQD setting gives a tremendous gain in scattered intensity of 7 relative to D11(11 m, 5.5 Å). The penumbra diameter projected on the moderator is 92 mm when R_1= 32 mm. Compared to D11(3.6 m, 4.5 Å), BLQD has approximately 15 % higher scattered intensity in the Q-range 0.007 - 0.12 $Å^{-1}$ and approximately 4 times better resolution over much of this range. Scattered intensity at the high Q-range (> 0.12 $Å^{-1}$) decreases by approximately a factor of 5 at 0.2 $Å^{-1}$ and 10 at 0.3 $Å^{-1}$ compared to D11(3.6, 4.5 Å); however, the resolution for BLQD still remains better than D11 by as much as a factor of 2. Only above a Q of 0.3 $Å^{-1}$ does the resolution become comparable then slightly worse than D11(3.6, 4.5 Å).The VLQD has approximately 35 % lower scattered intensity than D11(76 m, 12 Å) at the same resolution. It is not surprising that the gain from using time-of-flight is small considering that the wavelength band width is only 1.6 Å ; compare this to 3.64 Å for the BLQD. The VLQD bandwidth is comparable with the $\Delta\lambda/\lambda$ = 12 % FWHM obtained for D11. An intensity gain of 1.45 comes from the larger phase space sampled by the VLQD relative to D11.

We could place the same detector configuration on D11 as used in the design of BLQD and VLQD. In this case the Q_{max} for the three D11 settings shown in Figure 5 and 6 would approximately triple. When comparing BLQD and D11, the same three settings for D11 would still be needed to span the Q-range 0.002 - 0.4 $Å^{-1}$, except now the range would extent even further to around 0.9 $Å^{-1}$. Scattered intensity and resolution at any previous Q value would remain the same; however, intensity would taper off in a similar way as seen for BLQD and VLQD at the new higher Q values due to using an off-center detector arrangement.

We are currently investigating the design of a seven multiple-aperture configuration (with intermediate baffles to prevent crosstalk). This system would require larger samples (3 cm diameter), but would increase the intensity by five to seven-fold while retaining resolution.

3.3. Effects of source pulse width and pulse tail on performance

Simulations of various source configurations show that increased peak and integrated neutron flux in the pulse is achieved at the expense of longer pulse tails [2]. It is of interest to know what the effect of the source pulse width and pulse tail have on a δ scatterer at a particular Q value. We, therefore, used three different neutron sources with the BLQD geometry to see what the effect would be on a δ scatterer centered at a Q value of 0.1 $Å^{-1}$. The first source is the liquid H_2 moderator coupled with a 60 cm Be-90 cm Pb reflector, a 1000 μs pulse width, and 0.734 ms pulse tail used in the optimization calculations. This source is called the long pulse, strong reflector. The second source was a liquid H_2 moderator coupled with a 40 cm Be-110 cm Ni reflector, using a short proton pulse of width of 1 μs, and a decay time constant of 0.274 ms. This source is called the short pulse, weak reflector. The third source was a liquid H_2 moderator coupled with a 150 cm (∞) Be reflector, a proton pulse width of 1000 μs, and a decay time constant of 1.710 ms. This source is called the long pulse, infinite reflector. The results from using these three sources is tabulated in Table 2. One effect of using a long pulse and strong or infinite reflector is a wider spread in the instrument response function

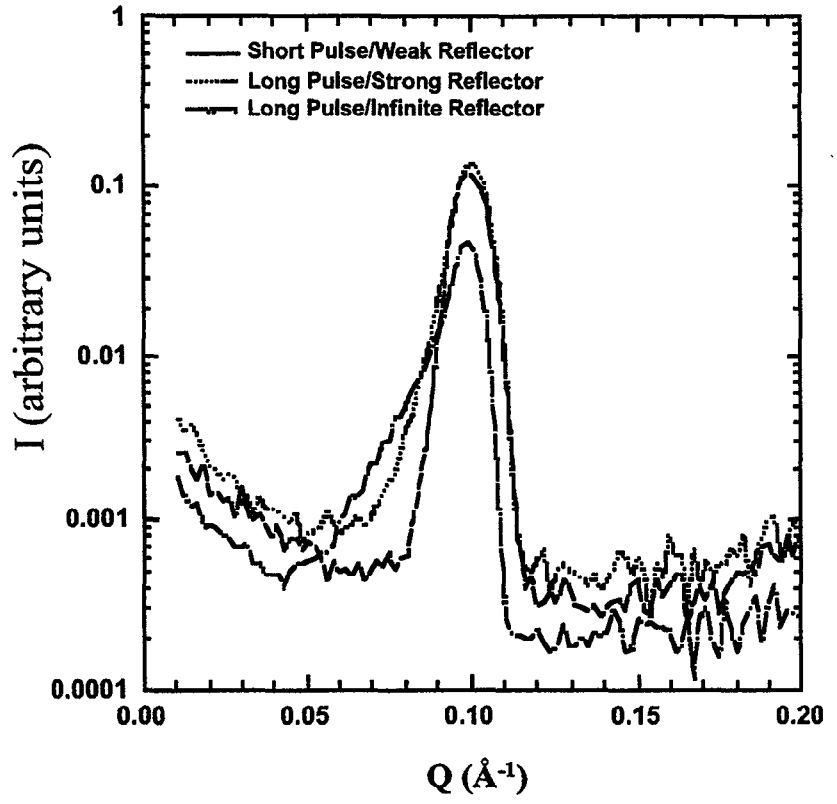

Figure 7. Effect on the resolution and scattering intensity from a d-scatterer using coupled moderator-reflector systems with different time constant in the exponential tail. BLQD is used in these simulations.

relative to the weak reflector, short pulse case (Fig. 7). This effect increases with Q and is quite apparent for $Q > 0.1$ Å^{-1} but is negligible for Q values < 0.05 Å^{-1}. The scattered intensity is highest for the long pulse, strong reflector suggesting that there is an optimal Be reflector thickness for the LPSS. The results indicate, further, that there is little to be gained by using a short pulse and weak reflector with this instrument.

Table 2.
Effects of Tails in Moderator-Reflector Configurations for a δ-scatterer on BLQD

	Reflector		
Parameter	40 cm Be, 110 cm Ni	60 cm Pb, 90 cm Be	Be (∞)
Proton Pulse Width (μs)	1	1000	1000
Moderator-reflector Time Constant (μs)	276	734	1710
Scattered Intensity ($MW^{-1}s^{-1}$)	8.95×10^6	1.15×10^7	4.31×10^6
Δλ (umbra) (Å)	3.56	2.92	1.56
Δλ (total) (Å)	3.96	3.64	3.64
σ rms @ Q=0.1 (Å^{-1})	0.0046	0.0056	0.0082

4. Conclusions

We optimized two instruments for a 1 MW LPSS operating at 60 Hz and a 1 ms proton pulse. In order to quantify the performance of these instruments, they were compared to D11 at the ILL. Scattered intensity gains between 3 - 7 for the BLQD over D11 were determined for the Q-range 0.0025 to 0.12 $Å^{-1}$. For $Q > 0.12$ $Å^{-1}$, scattered intensity for BLQD is lower than D11(3.6 m, 4.5 Å). However, the resolution is considerably better. We conclude that the two BLQD phase settings of λ_{max} = 10.2 and 6.4 Å can adequately cover the Q-range between 0.0025 - 0.44 $Å^{-1}$ and BLQD can perform better than D11 with regards to resolution and scattered intensity over most of this Q-range. The VLQD (λ_{max} = 12.8 Å) at the same resolution as D11(76 m, 12 Å) is approximately 35 % lower in scattered intensity. Because VLQD is only 36 m long, utilization of multiple aperture collimation on this instrument may be possible with an increase in scattered intensity by approximately a factor of 4 over D11(76 m, 12 Å). Similar gains can be expected if multiple aperture collimation is used on BLQD. Comparisons of the optimized instruments using long and short pulses and different reflectors suggest that there is an optimal moderator-reflector configuration, and that using a short pulse does not largely improve the performance of these instruments.

5. References

[1] Long Pulse Spallation Source Workshop, Berkeley National Laboratory, Berkeley, California, April 18 - 21, 1995.

[2] E.J. Pitcher, G. J. Russell, P.A. Seeger, and P.D. Fergusson,, "Performance of Long-pulse Source Reference Target-Moderator-Reflector Configurations" Proceedings of ICANS-XIII, Paul Scherrer Institut, Villigen, Switzerland, Oct. 11-14, 1995.

[3] P. A. Seeger, "The MCLIB Library: Monte Carlo Simulation of Neutron Scattering Instruments," Proceedings of ICANS-XIII, Paul Scherrer Institut, Villigen, Switzerland, Oct. 11-14, 1995.

[4] M. W. Johnson and C. Stephanou, "MCLIB: A Library of Monte Carlo Subroutines for Neutron Scattering Problems," Rutherford Laboratory report RL-78-090.

[5] P. A. Seeger and R. P. Hjelm, "A Very-Low-Q-Diffractometer for an Advanced Spallation Source," Proceedings of ICANS-XII, Abingdon, U.K., May 24-28, 1993.

[6] P. A. Seeger and R. P. Hjelm, "Design and Implementation of Low-Q Diffractometers at Spallation Sources," American Crystallographic Association Symposia Proceedings, Albuquerque, NM, May 24-28, 1993.

[7] P. A. Seeger, "Optimization of Geometric Resolution in Small-Angle Scattering," Nuclear Instruments and Methods 178, 157-161 (1980).

[8] P. A. Seeger and R. Pynn, "Resolution of Pulsed-Source Small-Angle Neutron Scattering," Nuclear Instruments and Methods in Physics Research A245 , 115-124 (1986).

[9] P. Lindner, R. P. May and P. A. Timmins, "Upgrading of the SANS instrument D11 ant ILL," Physica B 180 & 181, 967-972 (1992).